Available online at www.sciencedirect.com

ScienceDirect

journal homepage: http://www.elsevier.com/locate/rpor

Technical note

Improved error detection using a divided treatment plan in volume modulated arc therapy

Kazuo Tarutani[a,b,*], *Masao Tanooka*[a,c], *Hiroshi Doi*[a,d], *Masayuki Fujiwara*[a], *Masaki Miyashita*[b], *Kazufumi Kagawa*[b], *Norihiko Kamikonya*[b], *Koichiro Yamakado*[a]

[a] *Department of Radiology, Hyogo College of Medicine, 1-1 Mukogawa-cho, Nishinomiya, Hyogo 663-8501, Japan*
[b] *Japan Organization of Occupational Health and Safety Kansai Rousai Hospital, 3-1-69, Inabaso, Amagasaki, Hyogo 660-8511, Japan*
[c] *Department of Radiotherapy, Takarazuka City Hospital, 4-5-1, Kohama, Takaraduka, Hyogo 665-0827, Japan*
[d] *Department of Radiation Oncology, Kindai University Faculty of Medicine, 377-2, Ohnohigashi, Sayama, Osaka 589-8511, Japan*

ARTICLE INFO

Article history:
Received 6 May 2018
Received in revised form
9 October 2018
Accepted 27 December 2018
Available online 21 January 2019

Keywords:
Volume modulated arc therapy
Electronic portal imaging device
Setup error

ABSTRACT

Aim: We sought to improve error detection ability during volume modulated arc therapy (VMAT) by dividing and evaluating the treatment plan.
Background: VMAT involves moving a beam source delivering radiation to tumor tissue through an arc, which significantly decreases treatment time. Treatment planning for VMAT involves many parameters. Quality assurance before treatment is a major focus of research.
Materials and methods: We used an established VMAT prostate treatment plan and divided it into $12^{\circ} \times 30^{\circ}$ sections. In all the sections, only image data that generated errors in one segment and those that were integrally acquired were evaluated by a gamma analysis. This was done with five different patient plans.
Results: The integrated image data resulting from errors in each section was 100% (tolerance 0.5 mm/0.5%) in the gamma analysis result in all image data. Division of the treatment plans produced a shift in the mean value of each gamma analysis in the cranial, left, and ventral directions of 94.59%, 98.83%, 96.58%, and the discrimination ability improved.
Conclusion: The error discrimination ability was improved by dividing and verifying the portal imaging.

* *Corresponding author at*: Department of Radiology, Hyog College of Medicine, 1-1, Mukogawa-cho, Nishinomiya, Hyogo 663-8501, Japan.
E-mail addresses: kazuo@kansaih.johas.go.jp (K. Tarutani), tanooka@hyo-med.ac.jp (M. Tanooka), h-doi@med.kindai.ac.jp (H. Doi), m-fuji@hyo-med.ac.jp (M. Fujiwara), miyashita-masaki@kansaih.johas.go (M. Miyashita), kagawa-kazufumi@kansaih.johas.go.jp (K. Kagawa), kamikon@hyo-med.ac.jp (N. Kamikonya), yamakado47@gmail.com (K. Yamakado).
https://doi.org/10.1016/j.rpor.2018.12.002

1. Background

Intensity Modulated Radiation Therapy (IMRT) is a useful method that can increase dose to tumor tissue while decreasing dose to organs at risk (OARs).[1,2] Unlike IMRT, which uses a step-and-shoot technique, volume modulated arc therapy (VMAT) involves moving the beam source through an arc, which significantly decreases treatment time.[3,4]

In treatment planning for VMAT, control of fluence, dynamics of multileaf collimation (MLC), dose rate, and gantry rotation speed are important. Quality assurance (QA) before treatment is a major focus of research.[5–9] While these verifications improve the safety of VMAT, random and systematic irradiation uncertainty in each part of the course remain possible.[10] In conventional pretreatment QA, it is not possible to predict mechanical errors, inappropriate movement, or human error.[11,12] Therefore, dose assessment during treatment has been developed in multiple research facilities,[13–17] and has been commercialized.[18,19]

Ford et al.[20] conducted a validation with an electronic portal imaging device (EPID) during treatment and found multiple errors of "high-potential severity." Errors are detectable by predicting the internal change in vivo using EPID. From this, it is possible to manage the treatment course using the portal image.

Dose verification using an EPID has been developed as part of pre-treatment QA.[21,22] In dose validation during treatment, the EPID can identify Monitor Unit (MU) values and changes in the shape of the irradiation field. However, small fluctuations, such as setup errors, cannot be detected in the integrated portal image.[23]

2. Aim

In this study, we sought to improve discrimination ability by dividing and verifying VMAT treatment plans.

3. Materials and methods

We used standard equipment comprising a linear accelerator (True Beam®,Varian Medical Systems, Mountain View, CA, USA) using Eclipse Ver. 11 and Portal Dosimetry software and a flat panel type of amorphous silicon (aSi) (EPID®, Varian Medical Systems, Mountain View, CA, USA). A commercial pelvic phantom (ExacTrac® Verification Phantom, BrainLab, Feldkirchen, Germany) was used.

3.1. *Treatment plans*

Five treatment plans for prostate patients were prepared. We used 74 Gy for each patient with prostate cancer. CT planning images of the commercial pelvic phantom were acquired. We made this image supply structure information and performed calculation in the commercial pelvic phantom geometry.

3.2. *Procedure*

The procedure is shown in Fig. 1. We set up the treatment planning to divide the prostatic treatment plan of VMAT and the prostatic treatment plan into 12 sections, each covering 30° of the arc. With the phantom on the treatment couch, we used the EPID and acquired fluence data over the 360° arc. We used these data as the baseline. We subsequently generated error that simulated body movement. We divided one course of treatment plan into 12 sections and made a 1 cm phantom shift in 3 directions in every section.

First, EPID data of each section was acquired. EPID data of the section when the phantom was moved in each direction was also acquired. Next, we generated an integrated image including only one section for each error. The integrated method of the image used the function (create composite image) of the software of portal dosimetry. We compared the reference image with the integrated image and generated the error per section and acquired the portal image. We performed this using five different treatment plans.

In other words, we acquired 12 times with each image which we divided one time of image which we integrated as baseline data into. Furthermore, we acquired 36 times of images which generated an error in the cranial, lateral, and ventral direction. And we acquired 36 times of integration images which generated an error in each section. Therefore, at first we acquired 13 as a reference image in total. And we become 72 times of acquisition every 1 patient data. Because we acquired 5 patient data in total, we acquired 373 times of data in total.

We analyzed the portal image using the EPID and conducted a gamma analysis at a pass rate of 0.5 mm/0.5%.[24] We normalized to correct for the dose and position error of the flat panel alignment.

3.3. *Data analysis*

We used commercial software (Microsoft Excel®, Microsoft, Redmond, WA, USA) for data integration and analysis. The portal dosimetry software of the linear accelerator was used for a gamma analysis.

4. Results

The gamma pass rate was 100% (permission value 0.5 mm/0.5%) in the integrated image with an error in only one section (Table 1). However, identification of errors was possible when we divided and verified one course of treatment plan. From the results of the gamma analysis of one treatment plan, we found the distribution with the largest error (Fig. 3). This gamma distribution contained 81.7% falls at the maximum gamma pass rate and we confirmed an average of 96.7% falls among all patients (Table 1).

The results of the gamma analysis of the integrated images in which errors were generated according to direction are shown in a box-plot diagram (Fig. 2). Identification of the error from the integrated image was impossible from these results (100%). In contrast, the mean pass rate, which we divided a treatment planning and analyzed was cranial shift

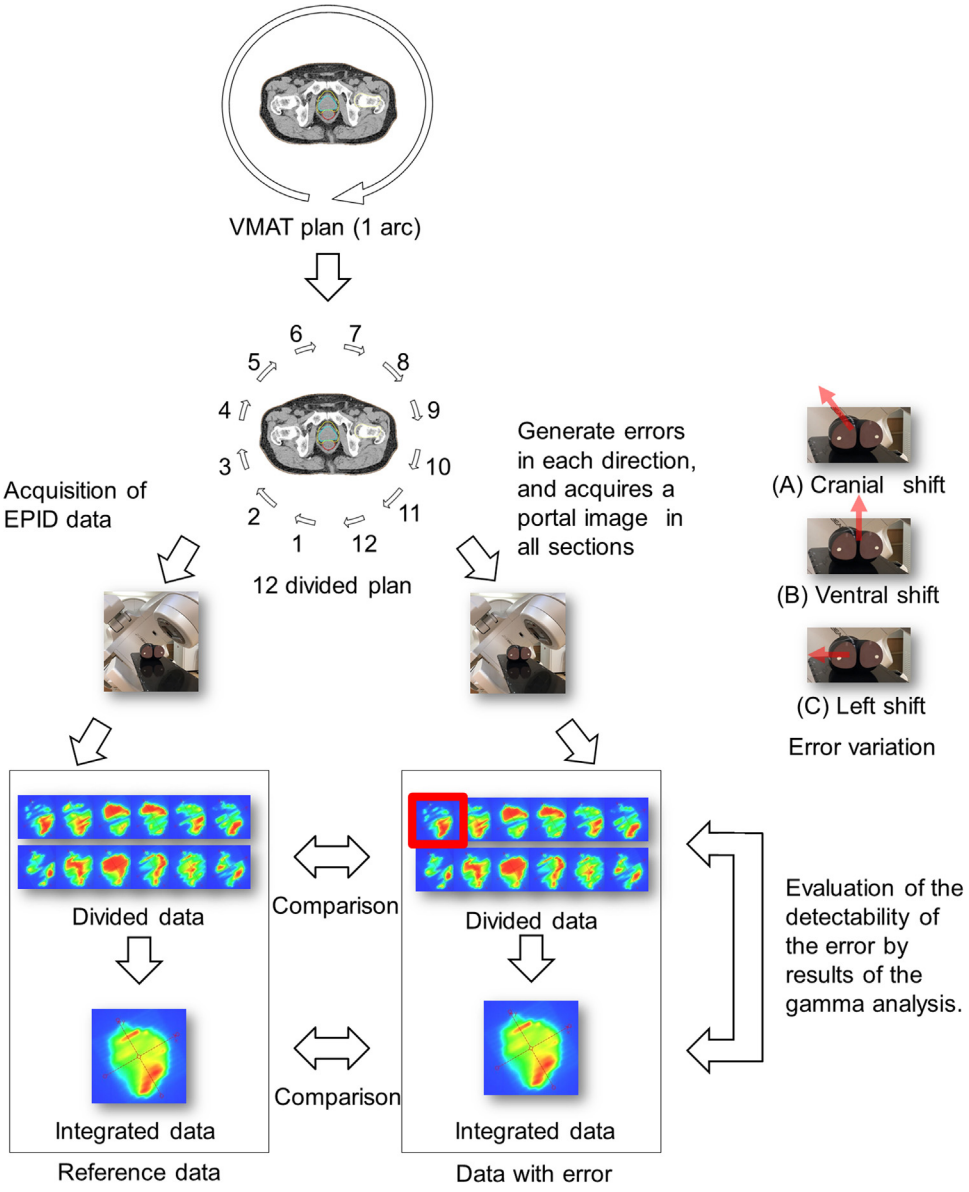

Fig. 1 – Chart of the workflow.

94.6%, lateral shift 98.8%, ventral shift 96.7% directions on the average, and the detection of error was possible.

The mean pass rate of the gamma analysis in the five patient plans was 96.8%, 96.0% 97.0%, 96.2%, and 97.4%. Then, we showed the identification ability that made a phantom shift to each direction (cranial, lateral, ventral). Average of the pass rate was 94.6%, 96.7% in the cranial direction, ventral direction, and the identification was possible. However, the pass rate in the lateral direction was 98.8%, and the identification ability was low (Fig. 4B). The identification sensitivity of the error differed by direction. It was 99.1% at the gamma pass ratio of the minimum detectability, and we were maximum, and it was 94%. The identification ability for the left shift was low.

5. Discussion

Dividing and verifying the treatment plan improved error discriminability. However, there is a variation of sensitivity by a generation direction of the error. It is thought that the cause is due to the generation direction of the error. In other words, we depend on a gantry angle and the generation direction of the error. It is thought that the identifiability of the error is influenced by patient's plan, part of the body, and direction. It is thought that it is influenced by the shape and area of the radiation field of the treatment plan. Therefore, identification of the error becomes possible in image data after many characteristics of the data are changed. We used an ExacTrac Verification Phantom in this study, but the results may vary

Table 1 – Results of gamma analysis of all patient groups (tolerance 0.5 mm/0.5%).

Section number		Cranial shift					
	Type	Patient 1	Patient 2	Patient 3	Patient 4	Patient 5	Mean
1 (180–210°)	Section only	97.8	91.9	95.7	96.7	99.0	96.2
	Integrated	100.0	100.0	100.0	100.0	100.0	100.0
2 (210–240°)	Section only	86.1	83.0	85.4	93.4	95.2	88.6
	Integrated	100.0	100.0	100.0	100.0	100.0	100.0
3 (240–270°)	Section only	94.7	82.1	99.0	92.0	87.0	91.0
	Integrated	100.0	100.0	100.0	100.0	100.0	100.0
4 (270–300°)	Section only	91.5	87.0	92.5	87.1	92.2	90.1
	Integrated	100.0	100.0	100.0	100.0	100.0	100.0
5 (300–330°)	Section only	96.6	89.8	94.1	91.9	97.6	94.0
	Integrated	100.0	100.0	100.0	100.0	100.0	100.0
6 (330–0°)	Section only	95.9	97.7	97.9	98.5	97.0	97.4
	Integrated	100.0	100.0	100.0	100.0	100.0	100.0
7 (0–30°)	Section only	98.9	95.9	93.6	99.6	99.7	97.5
	Integrated	100.0	100.0	100.0	100.0	100.0	100.0
8 (30–60°)	Section only	95.3	96.4	95.2	96.5	94.1	95.5
	Integrated	100.0	100.0	100.0	100.0	100.0	100.0
9 (60–90°)	Section only	97.6	94.4	94.3	95.3	99.2	96.2
	Integrated	100.0	100.0	100.0	100.0	100.0	100.0
10 (90–120°)	Section only	98.4	97.0	98.4	88.5	99.5	96.4
	Integrated	100.0	100.0	100.0	100.0	100.0	100.0
11 (120–150°)	Section only	94.6	97.1	91.1	91.2	95.6	93.9
	Integrated	100.0	100.0	100.0	100.0	100.0	100.0
12 (150–180°)	Section only	97.1	98.9	97.0	99.1	99.6	98.3
	Integrated	100.0	100.0	100.0	100.0	100.0	100.0
Mean	Section only	95.4	92.6	94.5	94.2	96.3	94.6
	Integrated	100.0	100.0	100.0	100.0	100.0	100.0

– Table 1 (*Continued*)

Section number		Left shift					
	Type	Patient 1	Patient 2	Patient 3	Patient 4	Patient 5	Mean
1 (180–210°)	Section only	99.3	99.8	99.8	99.8	98.7	99.5
	Integrated	100.0	100.0	100.0	100.0	100.0	100.0
2 (210–240°)	Section only	96.1	99.1	98.5	100.0	99.0	98.5
	Integrated	100.0	100.0	100.0	100.0	100.0	100.0
3 (240–270°)	Section only	99.9	99.8	99.8	99.9	99.5	99.8
	Integrated	100.0	100.0	100.0	100.0	100.0	100.0
4 (270–300°)	Section only	99.6	98.5	99.9	97.5	99.5	99.0
	Integrated	100.0	100.0	100.0	100.0	100.0	100.0
5 (300–330°)	Section only	96.8	99.1	99.4	94.8	99.3	97.6
	Integrated	100.0	100.0	100.0	100.0	100.0	100.0
6 (330–0°)	Section only	96.4	97.9	98.5	99.5	98.2	98.1
	Integrated	100.0	100.0	100.0	100.0	100.0	100.0
7 (0–30°)	Section only	100.0	99.3	99.8	99.9	99.6	99.7
	Integrated	100.0	100.0	100.0	100.0	100.0	100.0
8 (30–60°)	Section only	94.1	96.4	97.2	99.0	96.9	96.7
	Integrated	100.0	100.0	100.0	100.0	100.0	100.0
9 (60–90°)	Section only	99.9	99.3	99.9	99.4	100	99.7
	Integrated	100.0	100.0	100.0	100.0	100.0	100.0
10 (90–120°)	Section only	99.9	99.4	99.9	99.5	99.9	99.7
	Integrated	100.0	100.0	100.0	100.0	100.0	100.0
11 (120–150°)	Section only	99.0	99.1	97.0	97.8	99.5	98.5
	Integrated	100.0	100.0	100.0	100.0	100.0	100.0
12 (150–180°)	Section only	98.6	97.9	99.1	98.9	99.8	98.9
	Integrated	100.0	100.0	100.0	100.0	100.0	100.0
Mean	Section only	98.3	98.8	99.1	98.8	99.2	98.8
	Integrated	100.0	100.0	100.0	100.0	100.0	100.0

– Table 1 (*Continued*)

Section number		Ventral shift					
	Type	Patient 1	Patient 2	Patient 3	Patient 4	Patient 5	Mean
1 (180–210°)	Section only	100.0	100.0	100.0	100.0	100.0	100.0
	Integrated	100.0	100.0	100.0	100.0	100.0	100.0
2 (210–240°)	Section only	94.4	99.5	98.8	100.0	99.4	98.4
	Integrated	100.0	100.0	100.0	100.0	100.0	100.0
3 (240–270°)	Section only	92.3	93.0	94.1	94.8	81.7	91.2
	Integrated	100.0	100.0	100.0	100.0	100.0	100.0
4 (270–300°)	Section only	94.7	94.7	95.1	86.5	94.4	93.1
	Integrated	100.0	100.0	100.0	100.0	100.0	100.0
5 (300–330°)	Section only	95.6	98.7	98.4	92.9	98.6	96.8
	Integrated	100.0	100.0	100.0	100.0	100.0	100.0
6 (330–0°)	Section only	100.0	100.0	100.0	100.0	100.0	100.0
	Integrated	100.0	100.0	100.0	100.0	100.0	100.0
7 (0–30°)	Section only	100.0	100.0	100.0	100.0	100.0	100.0
	Integrated	100.0	100.0	100.0	100.0	100.0	100.0
8 (30–60°)	Section only	91.9	94.4	96.2	98.4	95.3	95.2
	Integrated	100.0	100.0	100.0	100.0	100.0	100.0
9 (60–90°)	Section only	94.7	88.7	92.4	90.9	98.4	93.0
	Integrated	100.0	100.0	100.0	100.0	100.0	100.0
10 (90–120°)	Section only	98.0	91.7	96.5	89.5	94.0	93.9
	Integrated	100.0	100.0	100.0	100.0	100.0	100.0
11 (120–150°)	Section only	99.0	99.6	97.9	96.0	99.7	98.4
	Integrated	100.0	100.0	100.0	100.0	100.0	100.0
12 (150–180°)	Section only	99.9	100.0	99.9	100.0	100.0	100.0
	Integrated	100.0	100.0	100.0	100.0	100.0	100.0
Mean	Section only	96.7	96.7	97.4	95.8	96.8	96.7
	Integrated	100.0	100.0	100.0	100.0	100.0	100.0

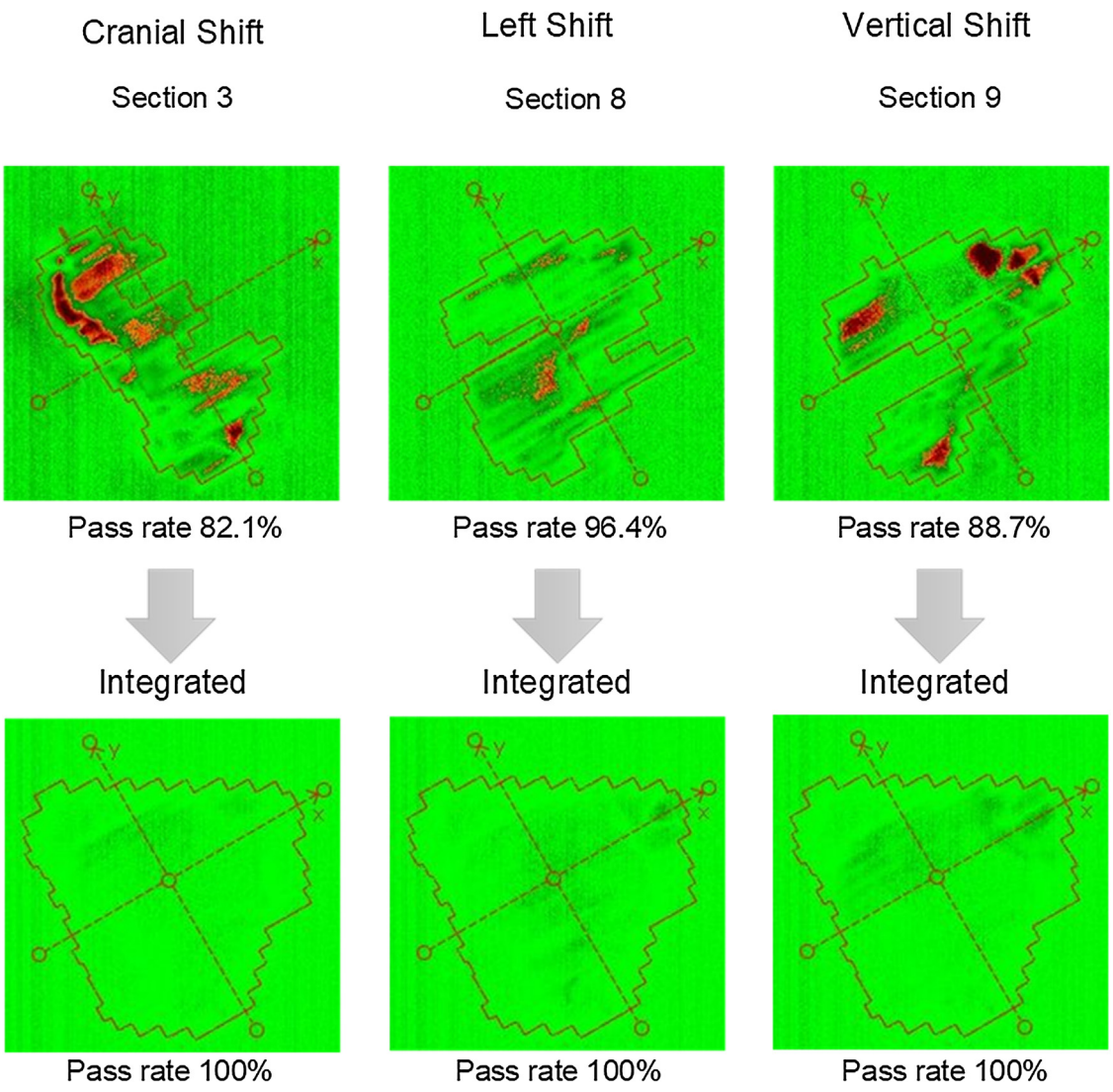

Fig. 2 – Example of distribution by gamma analysis (tolerance 0.5 mm/0.5% normalization point minimum value, auto alignment). While gamma analysis of divided image data could detect errors, this was impossible in integrated image data.

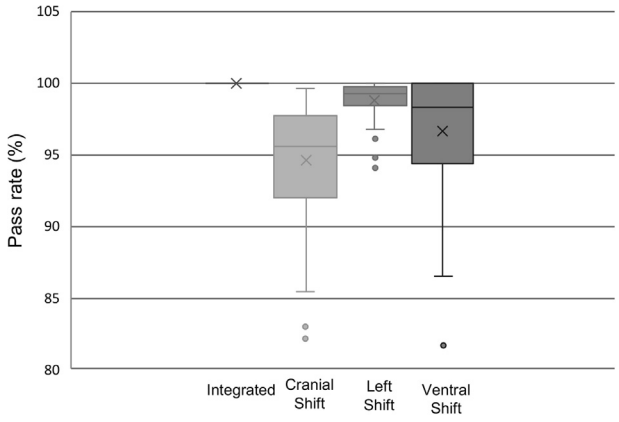

Fig. 3 – Box plot of gamma analysis of integrated image data and image data generating errors in each direction.

among parts of the body. For example, the improvement of detectability would be possible if it is a portal image which is transmitted for a body structure with a high quantity of characteristics. In clinical practice, temporal changes such as moving rectal gas[25,26] can induce large displacement errors. In such cases, the setup error may not be identifiable. In addition, the tolerance of the gamma analysis[24] was set to distance to agreement and the dose difference was 0.5 mm/0.5% respectively. The reason is to improve the sensitivity of the analysis result. If the tolerance is set low, the sensitivity of the error increases.[27] However, the result may contain noise and may not provide accurate results. Analysis methods and tolerance settings may be refined in future research.

Research into a system that monitors with EPID in real time is currently being conducted.[28] However, we predict that specifying the cause of errors will continue to be difficult.

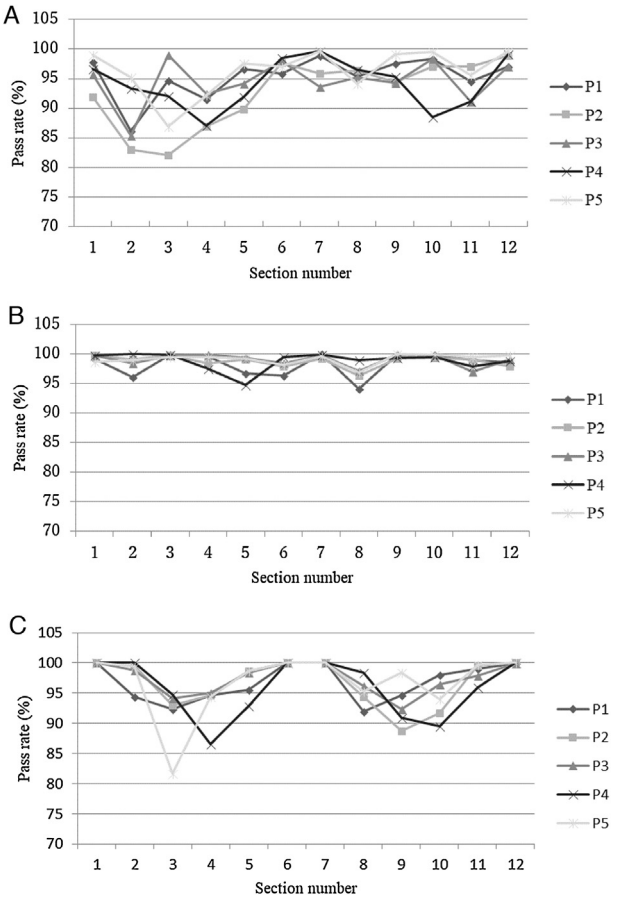

Fig. 4 – Gamma analysis result. (A) Cranial shift. (B) Left shift. (C) Ventral shift. P1–5 indicates the 5 treatment plans.

Currently, verification during treatment with VMAT using EPID is managed using portal imaging. In this study, we found that changes in movement during treatment were very likely to be blurred and undetectable, and were difficult to verify. The discrimination performance improved by dividing the image into $12^\circ \times 30^\circ$ segments. Therefore, it may be helpful to conduct verification in divided data for irradiation surveillance during treatment, which we showed increased sensitivity. However, actually, radiotherapy is not provided after dividing treatment plan. Therefore, we divide data during radiotherapy in real time, and a system to analyze at the same time is required. If it is enabled, errors such as mechanical or setup errors will be reduced but can predict that we use this method. Therefore, QA between the treatments is more useful than QA before the treatment if we divide EPID data and analyze it.

6. Conclusion

The error discrimination ability was improved by dividing and verifying the EPID data.

Conflict of interest

None declared.

This work was presented in part at the Japan-Korea Joint Meeting on Medical Physics 8th Annual Meeting in Osaka, Japan on September 15–17, 2017.

Financial disclosure

This research was conducted with the support of Hyogo College of Medicine and with the support of research funding to promote the hospital function of the Japan Industrial Safety and Health Organization.

REFERENCES

1. Staffurth J. Radiotherapy Development Board. A review of the clinical evidence for intensity-modulated radiotherapy. *Clin Oncol* 2010;**22**:643–57.
2. Viani GA, Viana BS, Martin JE, Rossi BT, Zuliani G, Stefano EJ. Intensity-modulated radiotherapy reduces toxicity with similar biochemical control compared with 3-dimensional conformal radiotherapy for prostate cancer: a randomized clinical trial. *Cancer* 2016;**122**:2004–11.
3. Yu CX. Intensity-modulated arc therapy with dynamic multileaf collimation: an alternative to tomotherapy. *Phys Med Biol* 1995;**40**:1435–49.
4. Otto K. Volumetric modulated arc therapy: IMRT in a single gantry arc. *Med Phys* 2008;**35**:310–7.
5. Defoor DL, Vazquez-Quino LA, Mavroidis P, Papanikolaou N, Stathakis S. Anatomy-based, patient-specific VMAT QA using EPID or MLC log files. *J Appl Clin Med Phys* 2015;**16**:5283.
6. Mijnheer B, Olaciregui-Ruiz I, Rozendaal R, Spreeuw H, van Herk M, Mans A. Current status of 3D EPID-based in vivo dosimetry in The Netherlands Cancer Institute. *J Phys Conf Ser* 2015:573.
7. Rowshanfarzad P, Mcgarry CK, Barnes MP, Sabet M, Ebert MA:. An EPID-based method for comprehensive verification of gantry EPID and the MLC carriage positional accuracy in Varian linacs during arc treatments. *Radiather Oncol* 2014;**9**:249.
8. Bojechko C, Phillps M, Kalet A, Ford EC. A quantification of the effectiveness of EPID dosimetry and software-based plan verification systems in detecting incidents in radiotherapy. *Med Phys* 2015;**42**:5363–9.
9. Vazquez Quino LA, Chen X, Fitzpatrick M, et al. Patient specific pre-treatment QA verification using an EPID approach. *Technol Cancer Res Treat* 2014;**13**:1–10.
10. Huang G, Medlam G, Lee J, et al. Error in the delivery of radiation therapy: results of a quality assurance review. *Int J Radiat Oncol Biol Phys* 2005;**61**:1590–5.
11. Mans A, Wendling M, McDermott LN, et al. Catching errors with in vivo EPID dosimetry. *Med Phys* 2010;**37**:2638–44.
12. Patton GA, Gaffney DK, Moeller JH. Facilitation of radiotherapeutic error by computerized record and verify systems. *Int J Radiat Oncol Biol Phys* 2003;**56**:50–7.
13. Wendling M, McDermott LN, Mans A, Sonke JJ, van Herk M, Mijnheer BJ. A simple backprojection algorithm for 3D in vivo

EPID dosimetry of IMRT treatments. *Med Phys* 2009;**36**:3310–21.
14. Mans A, Remeijer P, Olaciregui-Ruiz I, et al. 3D Dosimetric verification of volumetric-modulated arc therapy by portal dosimetry. *Radiother Oncol* 2010;**94**:181–7.
15. Olaciregui-Ruiz I, Rozendaal R, Mijnheer B, van Herk M, Mans A. Automatic in vivo portal dosimetry of all treatments. *Phys Med Biol* 2013;**58**:8253–64.
16. Fidanzio A, Azario L, Greco F, Cilla S, Piermattei A. Routine EPID in-vivo dosimetry in a reference point for conformal radiotherapy treatments. *Phys Med Biol* 2015;**60**:N141–50.
17. Rozendaal RA, Mijnheer BJ, Hamming-Vrieze O, Mans A, van Herk M. Impact of daily anatomical changes on EPID-based in vivo dosimetry of VMAT treatments of head-and-neck cancer. *Radiother Oncol* 2015;**116**:70–4.
18. Bailey DW, Kumaraswamy L, Bakhtiari M, Malhotra HK, Podgorsak MB. EPID dosimetry for pretreatment quality assurance with two commercial systems. *J Appl Clin Med Phys* 2012;**13**:3736.
19. Royer P, Marchesi V, Rousseau V, et al. Evaluation of transit in vivo dosimetry using portal imaging and comparison with measurements using diodes. *Cancer Radiother* 2014;**18**: 183–90.
20. Ford EC, Terezakis S, Souranus A, Harris K, Gay H, Mutic S. Quality control quantification (QCQ): a tool to measure the value of quality control checks in radiation oncology. *Int J Radiat Oncol Bio Phys* 2012;**84**:e263–9.
21. Talamonti C, Casati M, Bucciolini M. Pretreatment verification of IMRT absolute dose distributions using a commercial math formula EPID. *Med Phys* 2006;**33**:4367–78.
22. Warkentin B, Steciw S, Rathee S, Fallone BG. Dosimetric IMRT verification with a flat-panel EPID. *Med Phys* 2003;**30**:3143–55.
23. Bedford JL, Hanson IM, Hansen VN. Portal dosimetry for VMAT using integrated images obtained during treatment. *Med Phys* 2014;**41**:021725.
24. Low DA, Dempsey JF. Evaluation of the gamma dose distribution comparison method. *Med Phys* 2003;**30**:2455–64.
25. Ogino I, Uemura H, Inoue T, Kubota Y, Nomura K, Okamoto N. Reduction of prostate motion by removal of gas in rectum during radiotherapy. *Int J Radiat Oncol Biol Phys* 2008;**72**:456–66.
26. Kroonwijk M, Pasma KL, Quint S, Koper PC, Visser AG, Heijmen BJ. In vivo dosimetry for prostate cancer patients using an electronic portal imaging device (EPID); demonstration of internal organ motion. *Radiother Oncol* 1998;**49**:125–32.
27. Pulliam KB, Huang JY, Howell RM, et al. Comparison of 2D and 3D gamma analyses. *Med Phys* 2014;**41**:021710.
28. Fuangrod T, Greer PB, Woodruf HC, et al. Investigation of a real-time EPID-based patient dose monitoring safety system using site-specific control limits. *Radiat Oncol* 2016;**11**:106.